

Nucleationless Three-Dimensional Island Formation in Low-Misfit Heteroepitaxy

P. Sutter* and M. G. Lagally

University of Wisconsin–Madison, Madison, Wisconsin 53706

(Received 26 October 1999)

The formation of faceted three-dimensional islands during growth of low-misfit $\text{Si}_{1-x}\text{Ge}_x$ alloys on Si(100) has been investigated by low-energy electron microscopy. The formation of the islands in these alloy systems does not involve three-dimensional nucleation, but rather proceeds via a precursor array of shallow, stepped mounds on the surface that result from the inherent morphological instability of the strained alloy film.

PACS numbers: 68.35.Bs, 61.16.Bg, 68.55.-a

The mechanisms that control the self-assembly of coherent, faceted three-dimensional (3D) islands in lattice-mismatched heteroepitaxial systems have been the subject of recent intense interest. This interest is driven by the prospect of developing fabrication schemes for future semiconductor devices in which macroscopic or at least mesoscopic ordered arrays of nanoscale device building blocks—individual quantum dots—form spontaneously during epitaxial growth. A number of fundamental aspects of the growth of such 3D islands in heteroepitaxy, e.g., ripening of island arrays [1] and the evolution of the island shape with increasing film thickness [1–3] and during embedding by the matrix material in the growth of multi-layer films [4], are now well documented. Nevertheless, important stages in the evolution from a strained layer to a partially relaxed film with faceted 3D islands remain poorly understood.

A widely used theory for the transition from the 2D layer to the faceted 3D islands assumes that these islands form via a 3D nucleation process [5]. The elastic energy of the initially planar, strained layer (the “wetting layer”) increases with growing film thickness, until the system can lower its free energy by nucleating faceted 3D islands, thus relaxing part of the misfit strain at the expense of a somewhat increased surface free energy. Three-dimensional island nucleation is characterized by a misfit-dependent critical volume, V_c , above which 3D islands are stable against decay towards a planar film. The interplay of strain and surface energy would make such 3D nucleation an activated process with activation energy E_A [5]. In the growth of $\text{Si}_{1-x}\text{Ge}_x$ on Si(100), shallow (105) faceted “hut” islands [6] have been observed at the early stage of the transition from the 2D layer to 3D morphology, for a range of misfits ε corresponding to Ge concentrations $0.1 \leq x \leq 1$. It has been argued that the mechanism governing their formation should qualitatively be the same over this entire composition range [3], and that this mechanism is 3D nucleation. Nucleation requires large fluctuations to form clusters of critical size, and while nucleation may be plausible for high misfits (large ε , small V_c), it seems less plausible at low misfits, where the system is more likely to choose an easier kinetic route that avoids fluctuations to form clusters of critical size.

In this Letter we present results, obtained from real-time low-energy electron microscopy (LEEM) observations of the surface morphology evolution during growth, that demonstrate that the mechanism of initial faceted 3D island formation in strained-layer epitaxy of $\text{Si}_{1-x}\text{Ge}_x$ alloy layers on Si(100) does not involve 3D nucleation. At low misfits, faceted 3D islands form continuously, without a significant kinetic barrier, from cells defined by a quasiperiodic 2D array of bunched steps whose spacing also changes continuously to provide nonfaceted cell side-walls. Our results provide a natural link between two apparently different strain relaxation mechanisms, via the formation of surface ripples [7,8] or via the nucleation of faceted 3D islands [3,6]. At small misfits a ripple or cell-like corrugational pattern acts as a precursor to the formation of faceted 3D islands. Our results are particularly significant given the need for a high degree of order in arrays of self-assembled quantum dot islands for most applications that have been proposed. If the islands form by nucleation, the statistical nature of the nucleation process will invariably cause disorder in the position of islands in an array. With nucleationless islanding, perfect periodic arrays may form spontaneously under suitable growth conditions. We believe that our conclusions hold generally for heteroepitaxial systems whose initial strain relaxation mechanisms involve the formation of faceted 3D islands.

Our growth experiments were performed in a LEEM [9] equipped with Si_2H_6 and Ge_2H_6 sources. Si wafers with miscuts between 0.05° and 0.2° away from the (001) orientation were cleaned *in situ* by brief heating to 1250°C [10]. $\text{Si}_{1-x}\text{Ge}_x$ alloy layers were grown on these substrates at temperatures around 700°C and at a growth rate of ~ 8 monolayers (ML) per minute. The evolving surface morphology was monitored by bright-field LEEM. In this imaging mode the facets bounding the 3D islands appear dark on a brighter background caused by the (100) oriented wetting layer. The wetting layer itself can also give rise to significant contrast that roughly scales with the local density of monolayer steps: Large step-free areas appear brighter than regions with groups of closely spaced atomic steps [11]. To confirm the conclusions drawn on the basis of this contrast mechanism, LEEM observations were complemented *in situ* by low-energy electron

diffraction (LEED) and *ex situ* by atomic-force microscopy (AFM).

Figure 1 shows a sequence of bright-field LEEM images, recorded during the growth of a $\text{Si}_{0.75}\text{Ge}_{0.25}$ alloy layer on Si(100) at $T = 700^\circ\text{C}$. The sequence illustrates a surface morphology evolution that we generally observe in the growth of low-misfit $\text{Si}_{1-x}\text{Ge}_x$ on Si(100) at high substrate temperatures. A loss of LEEM contrast at an alloy thickness of a few atomic layers, which we attribute to monolayer roughness in the form of very small 2D islands [12], is followed by a gradual reappearance of the contrast in a quasiperiodic pattern of dark cells separated by a mesh of bright lines [Fig. 1(a)], corresponding to a modulated density of atomic steps across the surface: dark (bright) contrast in areas with high (low) step density. The period of the observed pattern (the cell size) scales inversely with Ge concentration in the alloy: An alloy layer with higher nominal Ge concentration produces a pattern of smaller cells. While the intervening bright lines (i.e., regions having low step density) hardly change with increasing alloy coverage, the cells themselves gradually become darker [Figs. 1(b)–1(d)]. This contrast evolution indicates an increasing step density within the individual cells, which—as we will show below—accompanies the formation and vertical growth of a mound at the position of each cell.

At the initial stages [Figs. 1(a) and 1(b)] LEED shows the well-developed diffraction pattern of a $2 \times N$ reconstructed (100) $\text{Si}_{1-x}\text{Ge}_x$ surface [13], which through the final stage [Fig. 1(d)] transforms into the characteristic LEED pattern of (105) faceted 3D hut islands [14]. The projected geometry of the cell pattern formed at the early stages remains unchanged through the formation of faceted 3D islands, i.e., the position and size of each member of the final array of faceted islands are defined at the very onset of cell formation. Most cells show a pronounced four-fold symmetry with straight edges aligned along [010] and [001] directions already at the early stages of their evolution. We believe that this symmetry of the cells can be explained by considering step interactions on strained layers, in a common framework with the step-bunching instability previously described for $\text{Si}_{1-x}\text{Ge}_x$ alloys in Si(100) [15]. We also observe in Fig. 1 that the LEEM contrast does not

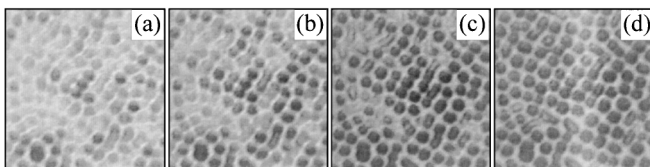


FIG. 1. Sequence of bright-field LEEM images of the growth of a $\text{Si}_{0.75}\text{Ge}_{0.25}$ alloy on Si(100) at $T = 700^\circ\text{C}$ (growth rate: 6 ML/min). Image (a) was recorded at 54 ML alloy coverage. The other images were taken after deposition of additional 6 ML (b), 12 ML (c), and 24 ML (d) of the $\text{Si}_{0.75}\text{Ge}_{0.25}$ alloy. The [010] and [001] directions are approximately along the image diagonals. Field of view: $2 \times 2 \mu\text{m}^2$.

develop uniformly across the imaged sample area. Rather, a few cells at first progress more rapidly than their surroundings, and the dark contrast then spreads from these forerunners to the neighboring cells. Significant differences thus exist initially in the density of steps in the individual cells [Fig. 1(a)]. The LEEM contrast at later stages shows that the evolution of cells with high step density slows down progressively. This behavior suggests that step interactions provide a self-regulation mechanism that causes the array to rapidly reach a state with equal step density in all cells.

The LEEM observations of Fig. 1 indicate that, in the growth of low-misfit $\text{Si}_{1-x}\text{Ge}_x$ alloy layers, faceted hut islands do not form by 3D nucleation on a planar wetting layer but rather grow out of a quasiperiodic array of “wedding-cake-like” mounds created from sets of monolayer-high steps. To corroborate this conclusion we performed AFM measurements on a sample whose growth was interrupted at an intermediate stage, corresponding to Fig. 1(b). AFM confirms the presence of an array of shallow protrusions on the surface with the periodicity of the cells observed by LEEM. Figure 2(a) shows an AFM micrograph of this sample in a representation in which different levels of gray characterize the slope of a surface element, i.e., the angle between the local surface normal and the [100] direction rather than the local surface height. The mounds are bounded by sidewalls with a continuous distribution of sidewall angles. The histogram in Fig. 2(b) shows a typical example: the upper limiting angle is that of the (105) facets bounding 3D hut islands. The distribution can be fitted to a broad normal distribution. Note the significant peak at $\sim 11^\circ$, where the mounds have transformed to (105) faceted hut islands and the absence of surface elements with inclination angles larger than 11° .

The combined LEEM and AFM results allow us to reconstruct the process of the formation of faceted 3D islands on low-misfit $\text{Si}_{1-x}\text{Ge}_x$ alloys on Si(100). A 3D surface morphology evolves first in the form of square

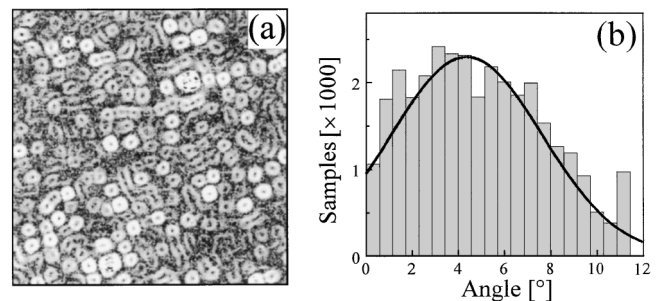


FIG. 2. Sidewall angles of evolving mound morphologies. (a) Atomic-force micrograph of the film shown in Fig. 1(b). Different levels of gray characterize the local slope of a surface element (black: 0° ; white: 11°). Field of view: $4 \times 4 \mu\text{m}^2$. (b) Histogram of the distribution of sidewall angles of the mounds shown in (a). The solid line is a fit to a normal distribution. Note the peak at $\sim 11^\circ$, corresponding to the slope of (105) facets and a lack of angles above 11° .

cells, bounded by bunched steps and arranged in a well-defined, quasiperiodic array on the surface. With continuing deposition, these mounds grow in height but not in their lateral size, which is limited by the presence of the neighboring features and thus remains constant at the initial value. The sidewall angle increases continuously until it approaches the angle of the (105) facet. At some point the surface can lower its free energy by converting the stepped mounds into (105) faceted hut islands.

Figure 3 shows a schematic plot of free energy E versus island volume V of films with a 3D surface morphology that either consists of stepped mounds or faceted hut islands. It illustrates why the observed continuous islanding process may be preferred over the 3D nucleation of faceted islands. We assume that the surface free energy of a vicinal SiGe surface increases linearly near the absolute minimum at (100) [16], and that it has a local minimum for the (105) facet orientation (i.e., there is a cusp in the Wulff plot). The free-energy curves shown in Fig. 3 mirror the tradeoff between (1) a positive surface free-energy term to create extra surface and (2) a strain relaxation energy, which reduces E for a 3D relative to a planar morphology [5]. The surface free-energy term causes the formation of a 3D morphology to be an activated process, characterized by a critical volume V_c and activation energy E_A . Both E_A and V_c scale with the sidewall angle of the mounds or islands: Less new surface is created when the morphology is shallower, hence the excess surface free energy is less, and the activation barrier is lower. The easiest evolutionary path for 3D island formation, shown by the dashed line, is one in which the mound angle (and thus the step density) increases continuously. It is essentially barrierless

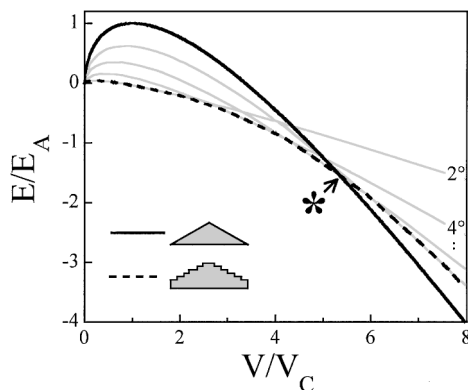


FIG. 3. Schematic plot of the free energy E [normalized to the activation energy E_A for nucleation of a (105) faceted hut island] as a function of island volume V (relative to the critical volume V_c of a hut) for an alloy film of constant composition and changing 3D morphology. The black line shows $E(V)$ for (105) faceted hut islands. Gray lines are $E(V)$ for mounds bounded by step bunches with fixed slopes. The dashed line is an envelope for all such curves for sidewall angles between 0° and 11° , and marks the evolution in free energy of a sequence of stepped mounds, which—initially shallow—grow continuously in height with increasing alloy coverage.

[17], and thus clearly favorable at the initial stages of the evolution of a 3D morphology. Implicit in the calculation of Fig. 3 is the likelihood that the surface free energy of the (105) facet is lower than that of a step bunch with the same slope ($\sim 11^\circ$) (or even of step bunches with somewhat smaller inclination angles), lowering the total free energy of faceted islands compared to mounds with the same or somewhat smaller inclination angles. There should then be a transition, driven by the desire to lower free energy, from a stepped mound to a faceted island at a well-defined point of the free-energy curve.

Our LEEM results clearly demonstrate that faceted 3D islands in low-misfit systems form without 3D nucleation, via a precursor of stepped mounds, but we have not yet discussed why the mounds themselves evolve from the initially planar alloy film. Here our results are linked with a previously proposed [7] and observed [8] morphological instability of strained epitaxial films: Epitaxial films subject to small misfit strain develop a biperiodic, sinusoidal “ripple” morphology, during growth or in a post-growth anneal. To elucidate this connection we recorded LEEM sequences during the growth of several $\text{Si}_{1-x}\text{Ge}_x$ alloy layers with different Ge concentrations x and used observations at the onset of mound formation to determine the dependence of the wavelength λ of the quasiperiodic cell pattern on misfit. Results of these experiments are shown in Fig. 4 for a range of Ge concentrations $0.14 \leq x \leq 0.4$. Our data indicate that λ decreases with increasing Ge content x or misfit ϵ , a trend in qualitative agreement with all theoretical models for the morphological instability of strained layers. From Fig. 4 we deduce $\lambda \propto \epsilon^{-(1.0 \pm 0.1)}$.

Our LEEM and AFM results are in obvious qualitative disagreement with simple models [8,18] that predict a functional form for the wavelength $\lambda(\epsilon)$ of the instability

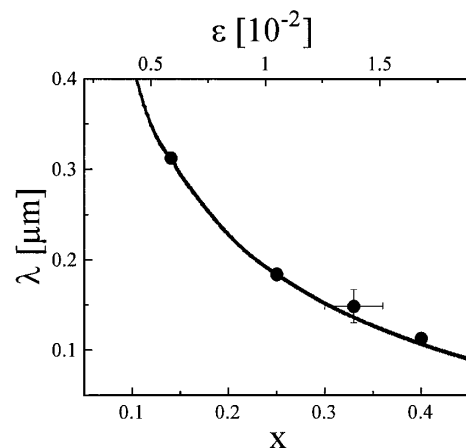


FIG. 4. Dependence of the wavelength λ of the initial cell pattern on Ge concentration, x , of the alloy film. Points denote values measured from LEEM images. The line is a calculation according to the model of Ref. [19], using a dimensionless growth rate $\nu = 10^{-3}$ and solute expansion coefficient $\eta^* = 0.5$.

of $t \propto \lambda^2 \cdot \varepsilon^2$, where t denotes the amplitude of the evolving 3D features. Our observations demonstrate that λ remains constant during alloy growth at constant composition ($\varepsilon = \text{const}$), while the height of the mounds continuously increases, i.e., we observe $\lambda^2 \cdot \varepsilon^2 = \text{const}$. Our data are inconsistent also with theoretical models of the morphological instability that take into account mass transport via surface diffusion or evaporation/condensation [7], but do not include a continuous flux of material onto the surface. In such a framework, which may capture the physics of an annealing or ripening experiment but not that of epitaxial growth, the maximally unstable wavelength is predicted to scale as ε^{-2} . The weaker ε^{-1} dependence observed in our experiments suggests that even a rather small growth flux can significantly stabilize the surface and shift the instability to longer wavelengths. A recent extended theory that includes surface diffusion, alloy decomposition, and epitaxial growth indeed predicts such a stabilization of the surface by a growth flux [19]. We employ the dependence on misfit of the maximally unstable wavelength for $\text{Si}_{1-x}\text{Ge}_x$ alloy growth on Si(100) predicted in Ref. [19], using appropriate values for the dimensionless solute expansion coefficient η^* (representing the change in lattice parameter as a function of alloy composition [20]) and dimensionless growth rate v [19] for comparison with our experimental results. Because we are interested only in the *functional form* of $\lambda(\varepsilon)$ predicted by theory, we scaled the calculated wavelengths λ to fit our experimental data. Figure 4 shows the agreement between our LEEM results and this calculation. We conclude that limitations caused by the growth flux and the energetics of the formation of arrays of stepped mounds can be understood within a framework of morphological instabilities of strained alloy films [19].

In conclusion, we have demonstrated that faceted 3D islands in the growth of low-misfit $\text{Si}_{1-x}\text{Ge}_x$ alloys on Si(100) do not form via 3D nucleation, but rather via a barrierless and continuous process involving a quasiperiodic 2D array of cells with bunched steps as sidewalls. The sidewall angle of these precursor cells increases continuously until the cells transform into faceted islands. Beyond this point the sidewall angle remains fixed at the (105) facet angle of 11° . This quasiperiodic roughness arises from the inherent morphological instability of a strained alloy film, but its nature, in particular, the wavelength of the roughness, is significantly affected by growth parameters, in particular, the deposition flux. We believe this mechanism holds generally for heteroepitaxial systems that involve the formation of faceted 3D islands.

This work was supported by ONR, NSF, and the Swiss National Science Foundation.

Note added.—It has come to our attention that similar LEEM observations of SiGe alloy roughening were recently obtained by Tromp, Ross, and Reuter [21].

*Permanent address: Department of Physics, Colorado School of Mines, Golden, CO 80401.

Email address: psutter@physics.mines.edu

- [1] F.M. Ross, J. Tersoff, and R.M. Tromp, *Phys. Rev. Lett.* **80**, 984 (1998).
- [2] G. Medeiros-Ribeiro, A.M. Bratkovski, T.I. Kamins, D.A.A. Ohlberg, and R.S. Williams, *Science* **279**, 353 (1998).
- [3] J.A. Floro, E. Chason, R.D. Twisten, R.Q. Hwang, and L.B. Freund, *Phys. Rev. Lett.* **79**, 3946 (1997).
- [4] P. Sutter and M.G. Lagally, *Phys. Rev. Lett.* **81**, 3471 (1998).
- [5] J. Tersoff and F.K. LeGoues, *Phys. Rev. Lett.* **72**, 3570 (1994).
- [6] Y.-W. Mo, D.E. Savage, B.S. Swartzentruber, and M.G. Lagally, *Phys. Rev. Lett.* **65**, 1020 (1990).
- [7] R.J. Asaro and W.A. Tiller, *Acta Metall.* **23**, 341 (1975); D.J. Srolovitz, *Acta Metall.* **37**, 621 (1989).
- [8] A.J. Pidduck, D.J. Robbins, A.G. Cullis, and W.Y. Leong, *Thin Solid Films* **222**, 78 (1992). For a recent review, see also A.G. Cullis, *MRS Bull.* **21**, 21 (1996).
- [9] R.M. Tromp and M.C. Reuter, *Ultramicroscopy* **36**, 99 (1991).
- [10] B.S. Swartzentruber, Y.-W. Mo, M.B. Webb, and M.G. Lagally, *J. Vac. Sci. Technol. A* **7**, 2901 (1989).
- [11] P. Sutter, E. Mateeva, J.S. Sullivan, and M.G. Lagally, *Thin Solid Films* **336**, 262 (1998).
- [12] M.G. Lagally, *Jpn. J. Appl. Phys.* **32**, 1493 (1993).
- [13] Y.-W. Mo and M.G. Lagally, *J. Cryst. Growth* **111**, 876 (1991); U. Köhler, O. Jusko, B. Müller, M. Horn von Hoegen, and M. Pook, *Ultramicroscopy* **42–44**, 832 (1991).
- [14] C.E. Aumann, Y.-W. Mo, and M.G. Lagally, *Appl. Phys. Lett.* **59**, 1061 (1991).
- [15] J. Tersoff, Y.H. Phang, Z. Zhang, and M.G. Lagally, *Phys. Rev. Lett.* **75**, 2730 (1995).
- [16] To obtain a qualitative understanding of the evolution of surface roughness via stepped mounds, we make a lowest-order approximation that neglects step interactions.
- [17] Our LEEM observations during alloy growth indicate that the surface is microscopically rough at the onset of mound formation, providing a high density of monolayer steps that can rearrange into the quasiperiodic cell patterns.
- [18] A.J. Pidduck, D.J. Robbins, and A.G. Cullis, in *Microscopy of Semiconducting Materials 1993*, edited by A.G. Cullis, J.L. Hutchison, and A.E. Staton-Bevan (IOP Publishing, Bristol, 1993).
- [19] J.E. Guyer and P.W. Voorhees, *Phys. Rev. Lett.* **74**, 4031 (1995); *Phys. Rev. B* **54**, 11 710 (1996).
- [20] F.C. Larché and J.W. Cahn, *Acta Metall.* **33**, 331 (1985).
- [21] R.M. Tromp, F.M. Ross, and M.C. Reuter, following Letter, *Phys. Rev. Lett.* **84**, 4641 (2000).